

THE SLAMMING OF 2-D SECTIONS ON THE WATER SURFACE AT CONSTANT AND VARIABLE DOWNWARD VELOCITY

Ismail Basaran^a, Omer Belik^b, Ozlem Akkus^b

^aKBR, Leatherhead, UK.

^bDepartment of Naval Architecture and Marine Engineering, Piri Reis University, Turkey

Abstract

In this study, a nonlinear numerical method is used to simulate the rigid body motion of a 2-D body penetrating the initially calm water surface at variable downward velocity, with the purpose of evaluating the resultant slamming force acting on the body. The flow around the body is modelled by the potential theory and the numerical solution is obtained by BEM. The validation of the numerical method is carried out by comparing the present results with those from the literature for wedges with different deadrise angles at constant downward velocity. The velocity profile of a body free falling in the water domain is calculated and compared with the available analytical and experimental results. In the present study, the temporal variation of the velocity is predicted at every time step simultaneously with the pressure variation. This is a definite improvement on other analytical solutions where the predetermined velocity profiles are imported into the pressure calculations.

Keywords: Slamming; water impact; BEM; free surface; hydrodynamic pressure

1. Introduction

The most severe hydrodynamic excitation on the ship structure is the transient slamming force. High forward speed and the sea state are the most important parameters determining the occurrence and severity of a slam. If the bottom of the ship emerges from the sea and returns by impacting on the free surface, “impact slamming” [1] is said to have occurred. This incorporates different physical phenomena happening at the same time, i.e. ventilation, air trapping, flow separation, etc. Impact slamming occurs within a very short time and may also be called “bottom slamming” [1]. The vertical velocity of the ship at the relevant section and the deadrise angle characterising the section are the main parameters of the impact slamming force. The faster a ship slams on the free surface and the lower deadrise angle it has, the higher impact pressure it sustains. As a body slams on the free surface in a free fall, its vertical velocity remains almost constant during the early stages of the impact. But the body decelerates while moving into the water because of the increasing displacement as well as the hydrodynamic force. Following the initial stages of

slamming, the physics of the phenomenon changes. As the body decelerates, the energy is transferred to the water and the water starts moving away from the body. The instantaneous vertical velocity and the shape of the body influence the amount of energy transferred to the water. During the energy transfer, the body suffers from a reaction force, designated as the “momentum force” and “momentum slamming” is said to have occurred [1], [2]. The ship structure endures major loading during momentum slamming. Especially, bow sections with high flare experience rapidly increasing momentum slamming forces [1].

In this study, both the early and later stages of the slamming of a simple 2-D body are investigated to obtain a nonlinear slamming force variation in time by a mathematical model and a numerical approach which deal with both “impact” and “momentum” slamming. Wedges with various deadrise angles at constant and variable downward velocities are studied and comparisons are made with the results of previous numerical and experimental studies.

The complex nature of the slamming has attracted attentions of many scientists. Von Karman's [3] and Wagner's [4] pioneering studies inspired researchers of the water entry problem. They both used the potential theory to predict slamming pressure on the body entering to the water. Wagner [4] tracked the water surface and tried to detect the intersection point between the free surface and the body, while von Karman [3] used simply a plate to represent the width of the section at the intersection points with the free surface. Dobrovol'skaya [5] studied the water entry of a wedge at constant velocity and presented a "similarity" analytical solution. She modelled the free surface jet flow and calculated pressures on wedges having different deadrise angles. Later Ochi and Motter [6] carried out a series of experiments to estimate "impact slamming" characteristics of ship bow sections. They assumed that the impact slamming

occured only over 0.1 of the draught from keel. Stovovy and Chuang [7] studied high speed vessels planing in waves. Considering the 3-D geometry at the point of impact and defining an effective impact angle with the water surface, they obtained a semiempirical expression for the slamming pressure. Belik et all. [1] made use of slamming theories in two different categories as "impact" and "momentum" slamming approaches and calculated the response of ships to slamming as well as cyclic wave excitation. Zhao and Faltinsen [8] improved Wagner's [4] theory by means of velocity potentials to represent the body and the water surface. They used the Boundary Element Method (BEM) to calculate the potentials on the body and the velocities on the water surface. They calculated the pressure distribution over the body by means of the Bernoulli equation.

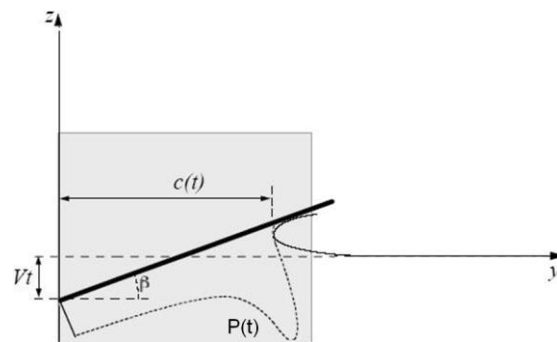


Fig. 1. The water entry model of Wagner [4].

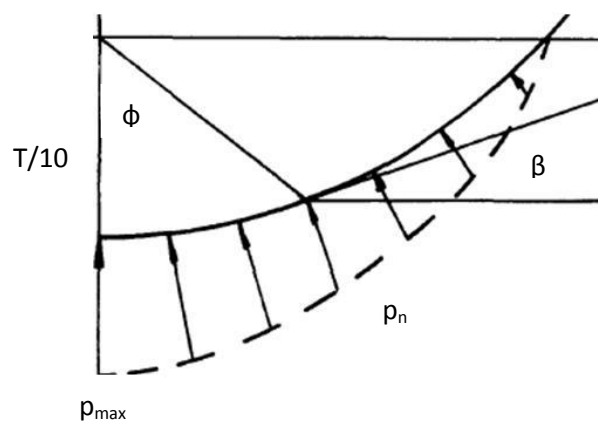


Fig. 2. The impact slamming model of Ochi and Motter [6]

Mei et all [9] modelled the slamming of ship sections by using the potential flow formulation of Wagner [4] and the Lewis transformations. Wu et all.[10] used complex potentials to solve the boundary value problem. They

simulated the free fall of a symmetric wedge on the water surface. Sun and Faltinsen [11] included the gravity in their calculations and introduced an approach to simulate the "water jet" development realistically. Kihara [12] similarly

used the BEM to investigate the bow slamming of a warship with a sonar dome placed at the hull bottom. Yettou et al [18] carried out an experimental study of free falling (variable downward velocity) wedges with deadrise angles varying from 15° to 35°.

2. Formulation of the problem

The fundamental aim of the present study is to obtain the hydrodynamic pressure on bodies penetrating water surface by executing a time domain simulation. In order to simulate slamming which comprises complex physics, it is necessary to make assumptions and idealisations. Slamming may conveniently be modelled in 2-D with a similar approach to the Strip Theory. Firstly, the fluid is assumed to be incompressible and nonviscous with irrotational flow so that potential flow can be applied. The acceleration of gravity is neglected since it is small compared to the body's inertia. The free surface of the water is assumed to be initially undisturbed. The possibility of trapped air being present during the impact is ignored. Possible hydroelastic effects are not accounted for as the body is assumed to be rigid.

A velocity potential $\Phi(y, z, t)$ is defined which satisfies the Laplace equation,

$$\nabla^2 \Phi(y, z, t) = \frac{\partial^2 \Phi}{\partial y^2} + \frac{\partial^2 \Phi}{\partial z^2} = 0 \quad (1)$$

The pressure on the free surface of the water is set to be the atmospheric pressure. The Bernoulli Equation,

$$p - p_a = -\rho \left(\frac{\partial \Phi}{\partial t} + \frac{1}{2} |\nabla \Phi|^2 + gz \right) \quad (2)$$

is reduced to the dynamic free surface condition

$$\frac{\partial \Phi}{\partial t} = -\frac{1}{2} |\nabla \Phi|^2 \quad (3)$$

by prescribing $p = p_a$ and omitting g . In the simulation however, as the change in the velocity potential is tracked at every time step, the material derivative of Φ , $(D\Phi/Dt)$ is used instead of the time derivative $(\partial\Phi/dt)$, since the potential variation is not only dependent on time but also on location. The material derivative operator for any function F is

$$\frac{DF}{Dt} = \frac{\partial F}{\partial t} + V \cdot \nabla F \quad (4)$$

If equation (4) is written for the velocity potential Φ and equation (3) is introduced in, the dynamic free surface condition is obtained as

$$\frac{D\Phi}{Dt} = \frac{1}{2} \left[\left(\frac{\partial \Phi}{\partial y} \right)^2 + \left(\frac{\partial \Phi}{\partial z} \right)^2 \right] \quad (5)$$

In addition, the displacement of the free surface at every time step has to be calculated. As the fluid particles cannot leave the free surface, the kinematic free – surface boundary condition can be written as

$$\frac{Dz}{Dt} = \frac{\partial \Phi(y, z, t)}{\partial z} \quad (6a)$$

$$\frac{Dy}{Dt} = \frac{\partial \Phi(y, z, t)}{\partial y} \quad (6b)$$

As the body touches the water surface, the boundary conditions change and the body boundary condition is to be taken into account thereof. On the wet body surface, the fluid flow has a velocity vector which has two components, normal and parallel to the body. The later is required for the pressure predictions. The former is expressed as the body boundary condition,

$$\frac{\partial \Phi}{\partial n} = V \cdot n \quad (7)$$

where n is the normal vector, positive outward from the fluid domain.

In order to solve the initial value problem, the initial conditions are required. Zhao and Faltinsen [8] assumed that the free surface of the water is not disturbed at the first penetration and velocity potential is equal to zero at the first step, $\Phi(y, z, t = t_0) = 0$. In this study, the free surface profile at the first step ($\zeta(y, t = t_0)$) is found using Wagner's [4] analytic solution,

$$\zeta(y, t = t_0) = \frac{Vt_0}{c} \arcsin\left(\frac{c}{z}\right) - Vt_0 \quad (8)$$

where

$$c = \frac{\pi V t_0}{2 \tan \beta} \quad (9)$$

is the half width of the wet body, β is deadrise angle and Vt_0 is the initial draught (or submergence). The initial perturbation into the water domain has to be selected large enough to avoid numerical errors. Finally, the initial conditions of the free surface are

$$\Phi = 0 \quad , \quad z = \zeta(y) \quad . \quad (10)$$

Using Green's second identity, a velocity potential on a point P is written as [13]

$$2\pi\Phi(P) = \int_{\Gamma} \left[G(P, q) \frac{\partial\Phi(q)}{\partial n_q} - \Phi(q) \frac{\partial G(P, q)}{\partial n_q} \right] d\Gamma \quad (11)$$

where

$$G(P, q) = -\ln r = -\ln|x_i - \xi_i| \quad (12)$$

and r is the distance between the loading and source points. Equation (11) is evaluated on the integration points over the body boundary, S_c , the free surface, S_s , and segments A and B (see Fig. 3). S_∞ is chosen sufficiently away from the body so that its contribution to the integral equation (11) is negligible. Greenhow [14] showed that a water jet occurs at the intersection point between body and the free surface. Zhao et al. [15] assumed that the contribution of the water jet to the pressure on the body is negligible and they incorporated in the calculation a cut off segment perpendicular to the body. In this work, a similar approach is used and the jet is cut off when the angle between the last element on the free surface and the first element on the body is smaller than a criterion, by introducing a "jet segment". At initial steps, the intersection points are found using mathematical expressions of the free surface and the body profile. The least squares method is used to obtain second order equations of the boundaries, taking into account 12 coordinates for the free surface and 6 coordinates for the body.

It must be pointed out that, although it is convenient for a wedge section, this procedure will be considerably more complicated when adopted for a ship section. In order to perform the calculations for a ship section, the number of coordinates for the body used in the procedure should be increased. It should be checked whether the intersection point

lies on the body boundary using a tolerance criterium. After the water jet is cut off, the intersection point between the jet segment and the body should be obtained using a similar procedure.

During the simulation, the "jet angle" is tracked at every time step. When the "jet angle" is smaller than a critical value, the jet segment is introduced. Following the initial introduction of the jet segment, the procedure is repeated every time an element on the free surface becomes almost parallel to body. The critical jet angle is chosen according to the wedge deadrise angle. For wedges with deadrise angles smaller than 45° the critical jet angle is chosen as 10° . Otherwise, it is 15° . For a more complex geometry such as a ship section, the critical jet angle will continuously vary with the changing geometry as the section penetrates the water surface.

The simulation is initiated by dividing the boundaries into linear elements. For simplicity, as the problem is symmetric about $z = 0$, only one half of the body and the free surface is considered. While the linear elements on the body boundary are equally spaced, the size of the elements on the free surface increase with square of the distance from the body. At the initial condition, the velocity on the body boundary, Eq. (7), and the potentials on the free surface are known, Eq. (10). The integral equation (11) is solved to obtain potentials on the body boundary elements and the normal velocities on the free surface elements. In the following step, the free surface is updated using the initial coordinates and the normal velocities. The normal velocities are obtained by solving the integral equation, whereas the tangential velocities are obtained separately. A central finite difference operator (Greco [16]) is used to calculate the tangential velocities by means of velocity potentials. In order to track the free surface, the following procedure is applied;

$$P(i, t + \Delta t) = P(i, t) + V(i, t) \cdot \Delta t \quad (13)$$

where, $P(i, t)$ is the i^{th} point at time t , $V(i, t)$ is the total velocity of the i^{th} point at time t and Δt is the time step. It is also necessary to update the potentials on the free surface in order to continue with the simulation. The dynamic free surface condition Eq. (5) is used to obtain the velocity

potential in the following step. When the water jet appears and cut off by the jet segment, the integral equation is also calculated on that segment. The potential on the jet segment is found by extrapolation, using first 5 elements on the free surface.

When the thickness of the jet segment is too large in comparison to the submergence of the body $V.t$ (when the

velocity is constant), the free surface becomes unstable, especially for deadrise angles higher than 45° . The jet thickness should also be monitored because of this reason. After many trials for both wedges and ship sections, it is concluded that keeping the ratio between the jet thickness and the submergence of the body δ less than 0.05 yields the best results. In order to keep the free surface stable,

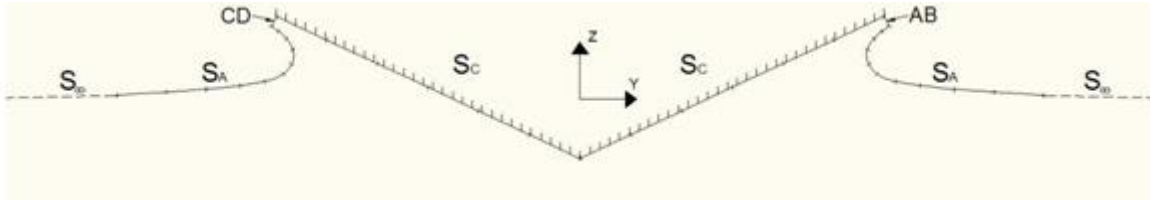


Fig. 3. Boundaries where integral equation is calculated for a wedge

when δ is equal or higher than 0.05, the free surface points are shifted to one point closer to the body. This procedure is formulated as follows:

$$P(i, t + \Delta t) = P(i - 1, t) + V(i, t) \cdot \Delta t \quad (13)$$

In order to prevent saw-teeth instability, a 5-node smoothing technique (Sun [17]) is deployed to fair the free surface coordinates and velocity potentials. Here the smoothing is repeated every 5th time step, although the frequency may be increased for higher deadrise angles. The velocity potentials on the body boundary are also calculated. By means of the Bernoulli Equation, Eq. (3), the hydrodynamic pressure is obtained. Since it is not possible to calculate $\partial\Phi/\partial t$ directly, the Bernoulli Equation is replaced by

$$\frac{\partial\Phi}{\partial t} = \frac{D\Phi}{Dt} - V \cdot \nabla\Phi \quad (14)$$

where V is the instantaneous velocity of the body and $\partial\Phi/\partial t$ is approximated as $\Delta\Phi/\Delta t$. $\nabla\Phi$ is calculated by fluid velocities in y and z directions. In order to calculate the fluid velocities around the body, a central finite difference operator (Greco [16]) is applied to velocity potentials on the body

boundary which are obtained by solving the integral equation, Eq. (11).

3. The validation of the dimensionless pressure coefficient for wedges at constant downward velocity

Wedges with various deadrise angles at constant downward velocity are investigated and results for different deadrise angles are presented in Fig. 4. Comparisons are made for the pressure coefficient obtained by the present study and by Sun and Faltinsen's [17] numerical model. The dimensionless pressure coefficient at the i^{th} segment on the body boundary is

$$C_p(i) = \frac{P(i, t)}{0.5\rho(V(t))^2} \quad (15)$$

where ρ is the fluid density, $P(i, t)$ is the pressure calculated at the i^{th} segment on the body boundary and $V(t)$ is the instantaneous velocity of the body at a time t . $V(t)$ is a function of time for a free falling body which leads to P and C_p being functions of time and space. However, if the velocity is constant, C_p is reduced to being only the function of space. Therefore, C_p calculated at any one segment must be identical for any two different time steps for a wedge falling at constant downward

velocity. In the numerical simulation, because the body boundary is discretised, there may be slight differences between results obtained at different time steps. As the simulation progresses, the number of segments in water increases and smoother C_p variation along the wedge is obtained. In Figs. 4, the X-Axes are the “dimensionless depth” which is equal to the Z-coordinate of the i^{th} segment $Z(i, t)$ divided by the instantaneous draft of the body.

$$\text{Dimensionless Depth} = Z(i, t)/V \cdot t$$

$V \cdot t$ is equal to the instantaneous draft of the wedge at constant velocity. The maximum value of C_p is found at the root of the water jet. This finding is valid for all ITUBEM’s results, for all deadrise

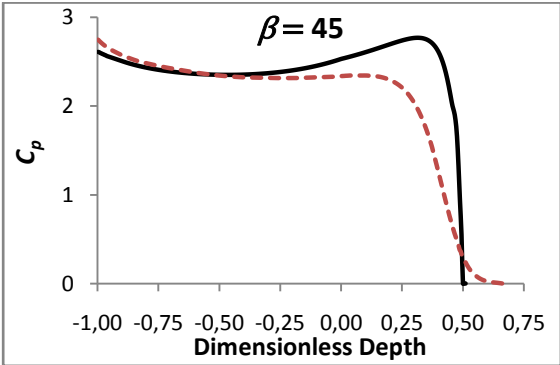
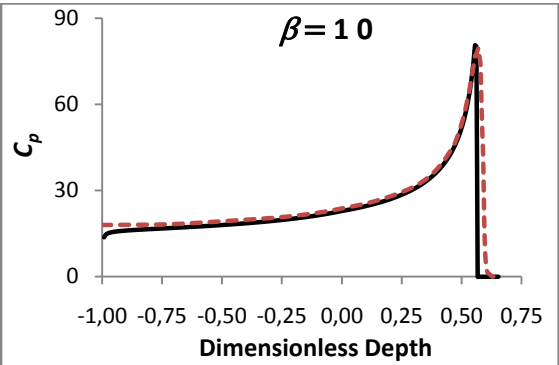
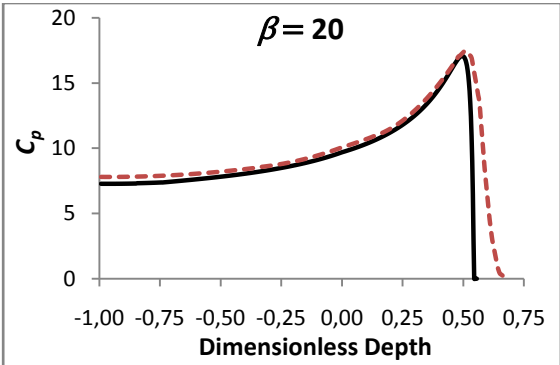
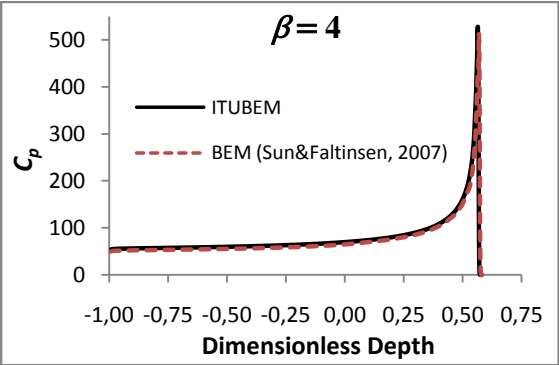
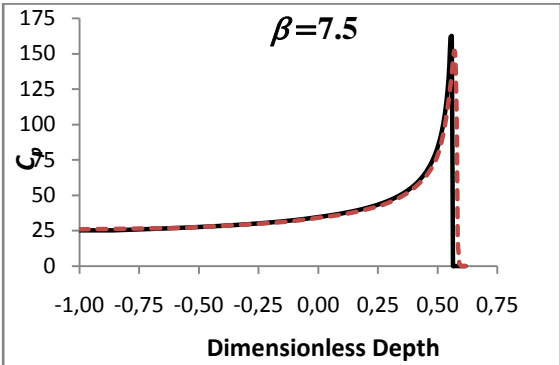
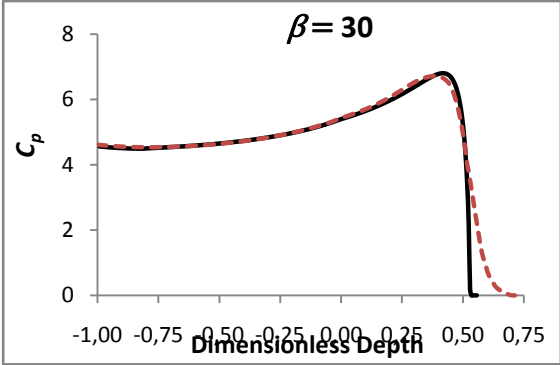


Fig. 4. Comparisons of the dimensionless pressure coefficient C_p calculated by Sun and Faltinsen [11] and the present study (ITUBEM) for deadrise angles 4° , 7.5° , 10° , 20° , 30° and 45° .

angles including $\beta=45^\circ$. But Sun and Faltinsen's [17] model predicts the maximum value of C_p at the bottom of the wedge for $\beta=45^\circ$. In general, comparisons are in good agreement. For small deadrise angles, peak values and the length of wetted surface are in noticeably good agreement. For deadrise angles higher than 10° , while peak values are in good agreement, the "wetted length" differs slightly. This difference is expected since, in the present study, the water jet is cut off as previously explained. For 45° deadrise angle, the peak value is overestimated compared to Sun and Faltinsen's [17] result. This trend is similar for higher deadrise angles, i.e. for $\beta > 45^\circ$. The higher the deadrise angle a wedge has, the harder it is to track the free surface and the water jet. It appears that the differences in the pressure predictions over the segments adjacent to the "jet segment" cause the discrepancy between the results and that the treatment of the water jet adopted here leads to higher pressure at around the root of the water jet. Sun and Faltinsen [17] used linear elements on the free surface and the body boundary while constant elements are used in the present study. The results also indicate that differences in the element size play a role in the differences in the predicted pressures, especially where the curvature of the free surface is high, i.e. at the root of the water jet (see Fig. 3).

From the structural engineering point of view, the discrepancies in the results for high deadrise angles are not likely to have a significant effect on the resultant total slamming force acting on a wedge or a ship section, mainly because the magnitude of the pressure coefficient is considerably smaller at high deadrise angles compared to those obtained for wedges with small deadrise angles. The main difference occurs at around the thin layer of the water jet which is excluded in the present study. It is expected that when integrating the pressure over

the "wetted length" in order to evaluate the slamming force, the thin layer of the water jet will not contribute significantly, since the pressure coefficient C_p is relatively small in that area. In Fig.4-e, it can be seen that, although the thin layer is not modelled by ITUBEM accurately, its contribution to the overall force is definitely small. In general, comparisons at constant downward velocity with different deadrise angles between results of ITUBEM and Sun and Faltinsen BEM [17] are encouraging enough to move onto simulations at variable downward velocity as explained in the following section as well as to apply the present method to arbitrary 2-D ship bow sections in the next study.

4. Comparisons of results for wedges at variable downward velocity between ITUBEM, experiments and analytical calculations

For the present purpose of meaningful comparisons between theory and experiment, the experimental results of Yettou et al [18] are used. They investigated the effects of the deadrise angle, drop height and total mass of the wedge on the water entry problem. Later, Yettou et al [19] also presented an analytical method to predict the pressure variation over the wedge. In this section, the results obtained by calculations (by ITUBEM) are compared with the experimental and theoretical results of Yettou et al [18], [19].

The drop experiment considered here was performed by a wedge with 25° deadrise angle and 94 kg mass, dropped from a height of 1.3 m on to the water surface. The pressure transducers were located at 12 points over the wedge to obtain the temporal and spatial pressure variation on the "wetted length". The distances between points were equally spaced at 50 mm (see Fig. 5). In the numerical simulation by ITUBEM, the coordinates of points where the pressure is calculated and presented in Fig.7 are chosen identical to the ones

in the experiment. The wedge is assumed to be at the same height from the water surface as in the experiment (i.e. 1.3 m) and the first impact velocity is evaluated by the energy conservation formula. The simulation is started as soon as the wedge touches the free surface. The time step is chosen small enough to track the free surface and the water jet correctly. The first 40 ms of the free fall is simulated and comparisons are made with the experimental results at 7 points of measurement.

In Fig. 6, the temporal variations of pressure and comparisons with experimental data are presented for 7 points on the face of the wedge. The experimental data are sampled from the original paper of Yettou et al [18].

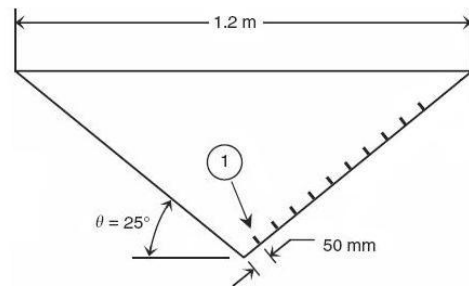
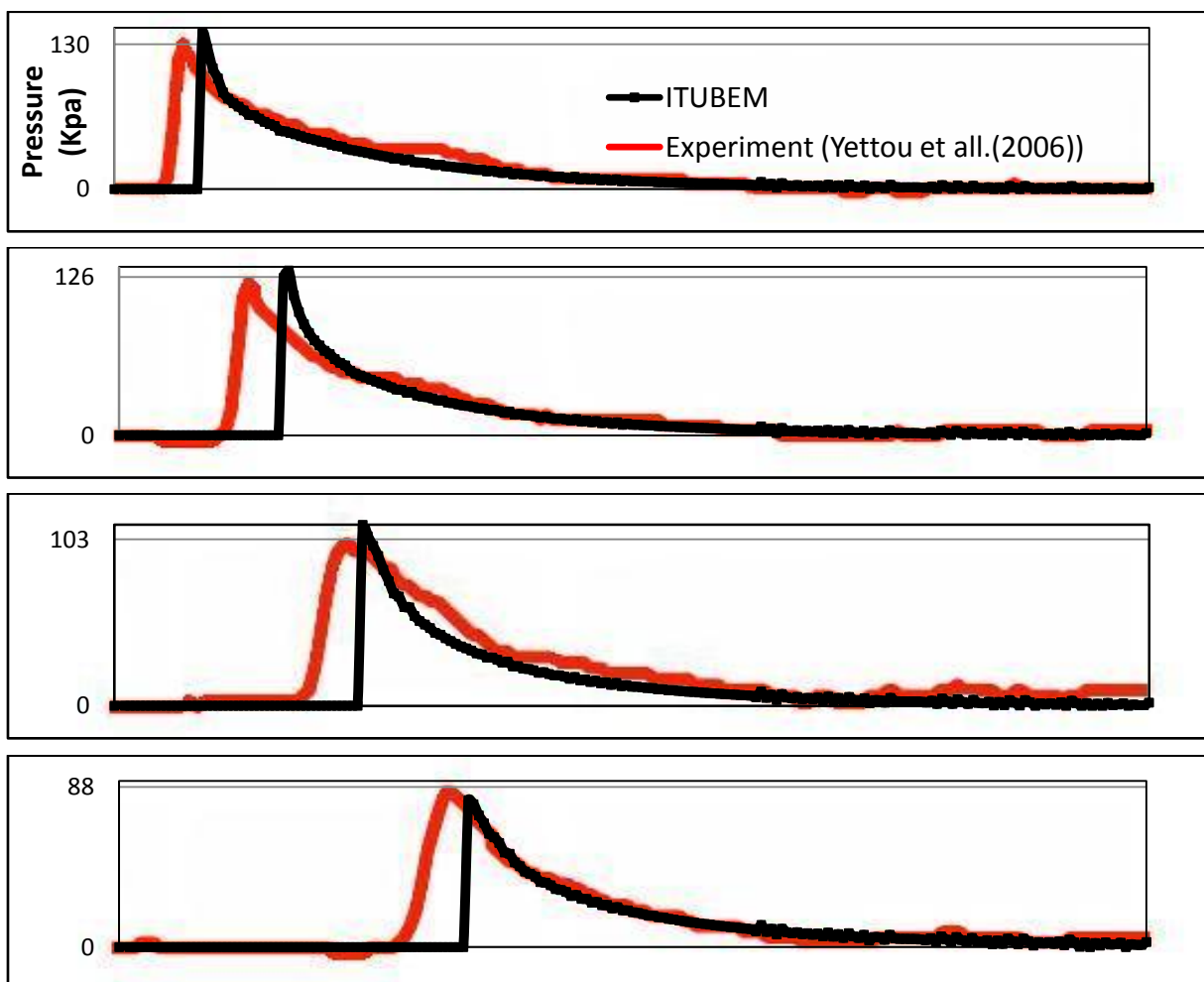


Fig.5. The positions of the pressure transducers in the experiment [18].

In general, the agreement between the measured and the predicted results is good. The general trend of the pressure variation in time is in good agreement for all points. The initial impact at each



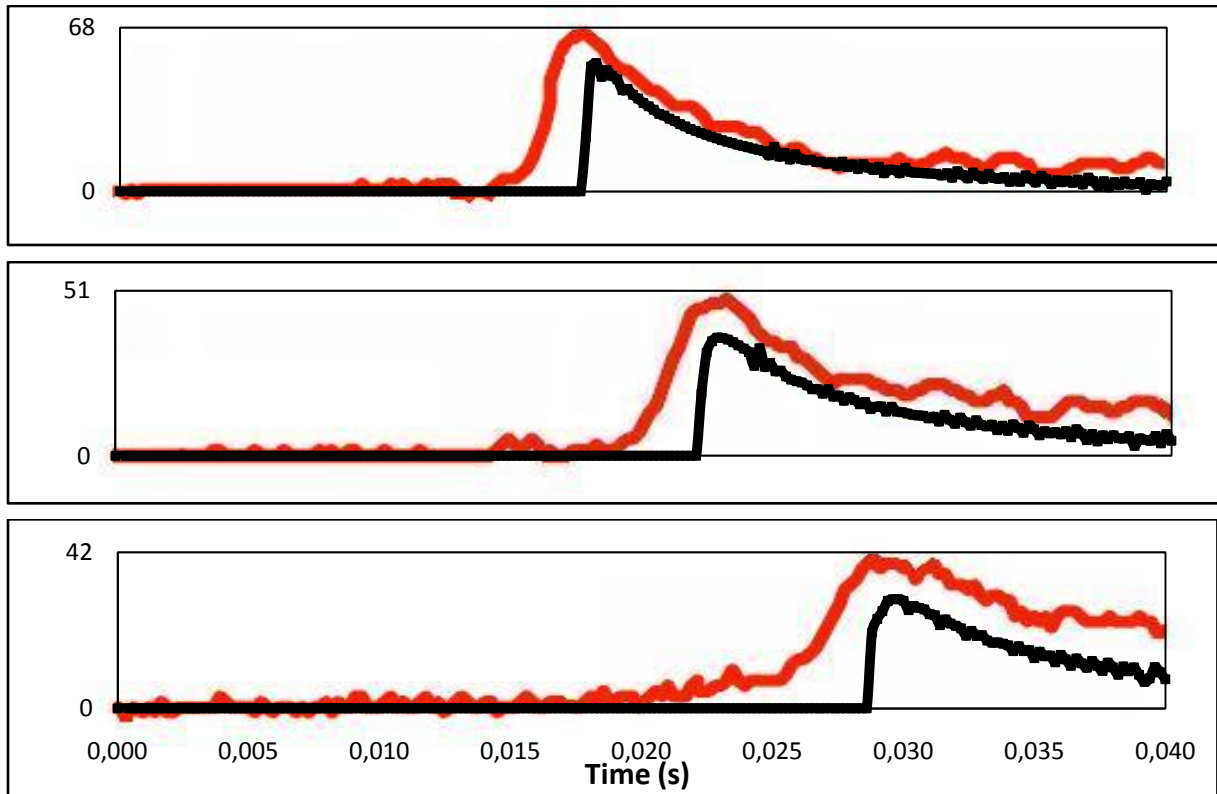


Fig. 6. Comparisons of measured [18] and calculated (ITUBEM) temporal pressure variation at seven points on the wedge with 25° deadrise angle.

point, the pressure peaks steeply to a maximum value. In the earlier stages of wedge impact, the peak is reached almost instantaneously. As the wedge further penetrates the water surface, both calculated and measured results show not only a drop in the peak pressure value, but also the maxima are reached more slowly compared to the steep peaks of initial stages of impact. The main difference between calculations and measurement occurs at the earlier stage for both the peak value and its timing. It can be seen that the timing of the impact is delayed but later calculated and measured results coincide. The timing delay can only be explained by the velocity profile of the free falling wedge which will be discussed later. The peak values are overestimated in the earlier stage of the slamming, while they are underestimated in the later stage. It should be noted that the impact is a very fast event and the differences in time are in the order of 0.001 s. For example, after 0.01 s

following the initial impact, both the peak values and the timing tend to agree. At approximately 0.02 s, the calculations start predicting lower pressure values. The numerical simulation, in general, predicts the immersion of a measurement point later than experiment. When the peak pressure value is high, the difference between the measured and predicted “immersion timing” is relatively small. The reverse is observed as the peak pressure value decreases. This discrepancy is thought to be due to the longer thin layer of water jet in the later stages of wedge immersion. As it is explained in the previous sections, in the simulations, the thin layer of the water jet is cut off for the sake of numerical stability.

The results presented and discussed above are obtained for a free falling wedge and the instantaneous velocity is calculated during the simulation at every time step. The vertical slamming force F_z per unit length of the wedge is

evaluated by integrating the pressure over the face of the wedge:

$$F_z = \int_0^l (P(s, t) + \rho g Z(s, t)) ds \cdot \cos\beta \quad (16)$$

Here, $P(s, t)$ is the hydrodynamic and $\rho g Z(s, t)$ is the hydrostatic contribution in Eq.(16). The latter is relatively small in the earlier stage of the slamming while it influences the total force and the velocity profile marginally in the later stage. Once the vertical slamming force is obtained, the acceleration of the body can be calculated. The equation of the rigid body motion is given by

$$M \frac{dV(t)}{dt} = F_z - mg \quad (17)$$

where M is the mass, $V(t)$ is the instantaneous velocity of the wedge and g is the gravitational acceleration. In the following time step, the velocity of the wedge which is predicted by this method is used in the integral equation, Eq. (11).

Yettou et al [19] used Zhao's model [15] to evaluate the velocity profile in time to calculate the pressure on the wedge analytically. Zhao's analytical model [15] is based on how "added mass" changes in time.

Utilising the momentum theorem, the velocity profile can be evaluated by

$$V(t) = \frac{V_0}{1 + M_a/M} \quad (18.a)$$

$$M_a = C_a \rho (Y(t))^2 \quad (18.b)$$

$$C_a = \frac{\delta \pi}{2} \left(1 - \frac{\beta}{2\pi}\right)^2 \quad (18.c)$$

where V_0 is the initial velocity at impact, M is the mass and M_a is the added mass of the wedge. $Y(t)$ is the maximum wetted width of the wedge at a time step t . δ is a correction factor which varies from 0.5 to 1 as defined in Zhao et al [15] and Meyerhof [20]. Once the velocity profile is obtained, the pressure variation can be evaluated analytically by Yettou's method [19] for a free falling wedge.

The experimental and analytical results for two different wedges are compared with the results of ITUBEM simulations. The first wedge has a 15° deadrise angle and a total mass of 143 kg. The second wedge has a 25° deadrise angle and a total mass of 94 kg. Both wedges have a square top of 1.2 m x 1.2 m. They are released from a height of 1.3 m above water level.

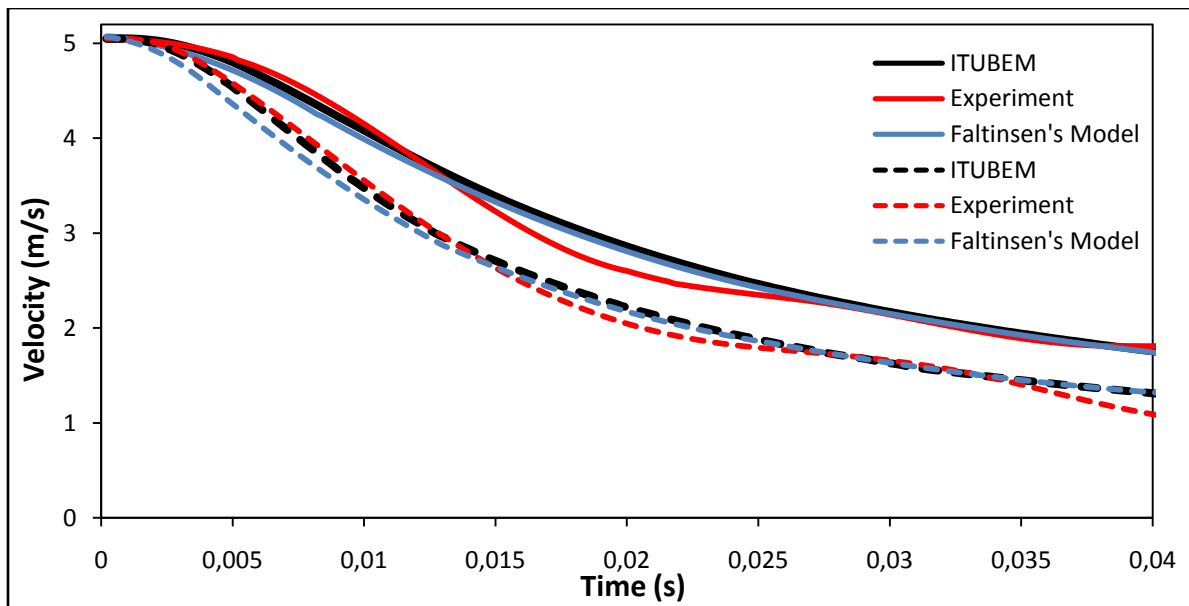


Fig.7. The variation of vertical velocity in time after impact for wedges with $\beta = 15^\circ$ (Dash lines) and 25° (Solid lines)

In Fig. 7, the experimental and analytical results from Yettou et al [18] are compared with the results of the present study (ITUBEM) for two different wedges described above. After the initial impact, the velocity of the wedge decreases rapidly. At the very early stage, the velocity remain almost unchanged for a very short period, followed by the relatively fast reduction. Zhao's model (Faltinsen in the figure) predicts faster reduction in the vertical velocity compared to both the experiments and ITUBEM simulations until about 0.015 s after the initial impact. Especially for the wedge with 15° deadrise angle, ITUBEM shows good agreement with the experiment until $t = 0.015$ s. In the later stages of the simulation, the ITUBEM calculations agree with the results of Zhao's model closely. Both comparisons for 15° and 25° deadrise angles show similar trends.

The “added mass” of the wedge is included in Zhao's model. It is not included in the rigid body motion by ITUBEM explicitly. The effect of the added mass is implicitly present in the hydrodynamic pressure that is calculated directly by the nonlinear boundary element method, in which the momentum conservation is satisfied. Sun [17] showed that after the flow separation at a discontinuity on the body, the hydrodynamic force

reduces rapidly (see Fig.8, at around $t = 0.0175$ s). Sun [17] also indicated that when the mass of the body is small relative to the added mass in the vertical motion, numerical problems may occur and the errors in the calculation of the acceleration may cause divergence. When such an error is encountered, the added mass is corrected numerically by Sun [17].

A comparison is made between Sun's and ITUBEM simulation results and the acceleration profile of a free falling wedge with 30° deadrise angle is presented in Fig. 8. The wedge has a mass of 10 kg and it is dropped from a height of 0.5 m. The variation of the acceleration computed by Sun [17] shows a sudden reduction after the flow separation, at which point a correction is introduced to the calculation procedure as explained above. The reduced acceleration is thought to be due to higher added mass after the flow separation. Remembering that the added mass is not explicitly included and the flow separation is not modelled by the present method (ITUBEM), the results are found to be in good agreement especially for the peak value and the variation in time. The time difference for the peak acceleration is only 0.0015 s and it is due to Sun [17] employing Wager's [4] analytical method in the initial stage of the calculations.

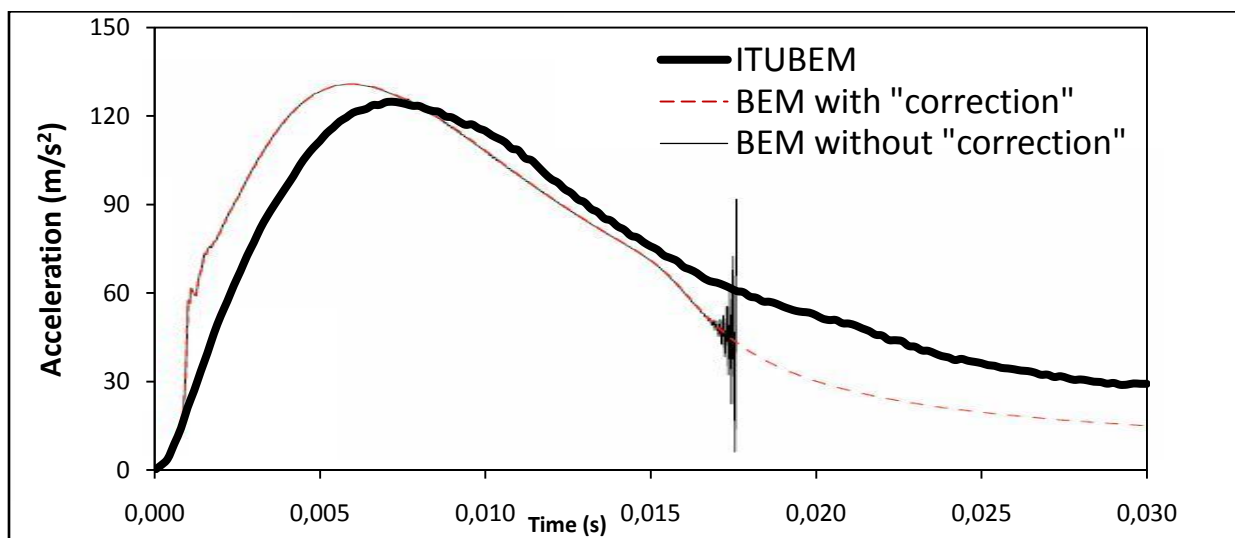


Fig. 8. The effect of the added mass on the acceleration after the flow separation [17].

Total slamming force acting on the wedge entering into water is calculated as explained in Eq. (16). For the sake of the comparisons with experimental results, hydrostatic pressure is also included in the calculation. In general, acceleration of the rigid body is very large relative to the gravitational acceleration. But the difference reduces rapidly and the hydrostatic pressure becomes influential at the later stage. In Fig. 9, ITUBEM's and experimental results of the resultant slamming force for a wedge with $\beta = 15^\circ$ and $m=143$ kg are presented. Both graphics are smoothed with 5-digit smoothing technique. The experimental result of the slamming force is derived from the velocity profile of the wedge in time.

$$F_z = M \frac{dV(t)}{dt} \tag{19}$$

The comparison of results at the early stage shows a very good agreement. After the maximum value is reached, both curves reduce rapidly. Results start showing different trends when $t = 0.02$ seconds. It can also be observed in the velocity profiles (see Fig. 7). In the experiment, the wedge decelerates less than the one in ITUBEM's simulation after $t = 0.02$ seconds while it decelerates more than the simulation after $t = 0.025$ seconds. That causes the differences in the comparison of the resultant slamming forces. On the other hand, total areas under two curves show a very good agreement. As the total force times time is related to the total momentum, one can say that total momentum is conserved by ITUBEM compared to the experiment.

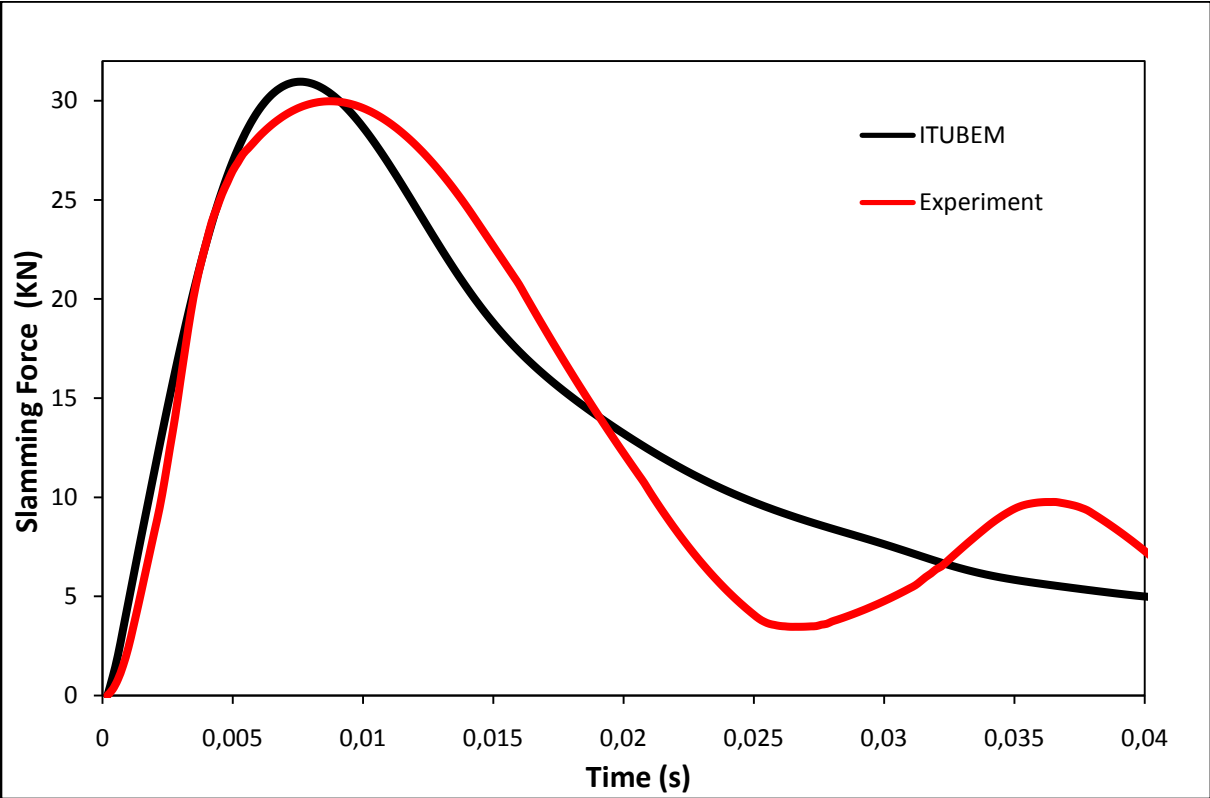


Fig. 9. Comparisons of the resultant slamming forces for a wedge with $\beta = 15^\circ$ and $m=143$ kg.

5. Conclusion

A non-linear Boundary Element Method (ITUBEM) has been developed to investigate the

slamming on the water surface of arbitrary 2-D sections at both constant and variable velocities. In

the present study, only 2-D wedges entering into the water surface have been studied.

First of all, comparisons were made with Sun and Faltinsen's [11] improved BEM for a wedge at constant downward velocity. Deadrise angles of wedges vary from 4° to 45° . Comparisons show a good agreement up to 45° deadrise angles. Discrepancies between results for deadrise angles higher than 10° are believed to be based on the different treatments of water jet.

Secondly, free falling wedges on the water surface have been simulated by ITUBEM. Experimental, analytical and numerical results from previous studies have been sampled for comparisons. Pressure variations measured by transducers in the experiments is also evaluated by ITUBEM. Although there some differences in the timing of

wetting, a good agreement happens in peak values and trends. Velocity profiles of wedges with two different deadrise angles and mass have been compared and show good agreements with experimental, analytical and numerical results. The resultant slamming force which is predicted by ITUBEM shows a very good agreement with the experiment at the early stage. Discrepancy between results at the later stage is believed to be related to ignored physical phenomena such as viscosity, splashes, etc. The gravitational acceleration may also play an important role in the discrepancy at the later stage when the acceleration of the free surface of the water is small relative to the early stage. It is believed that total areas under the curves for both results show a good agreement in terms of the conservation of the total momentum.

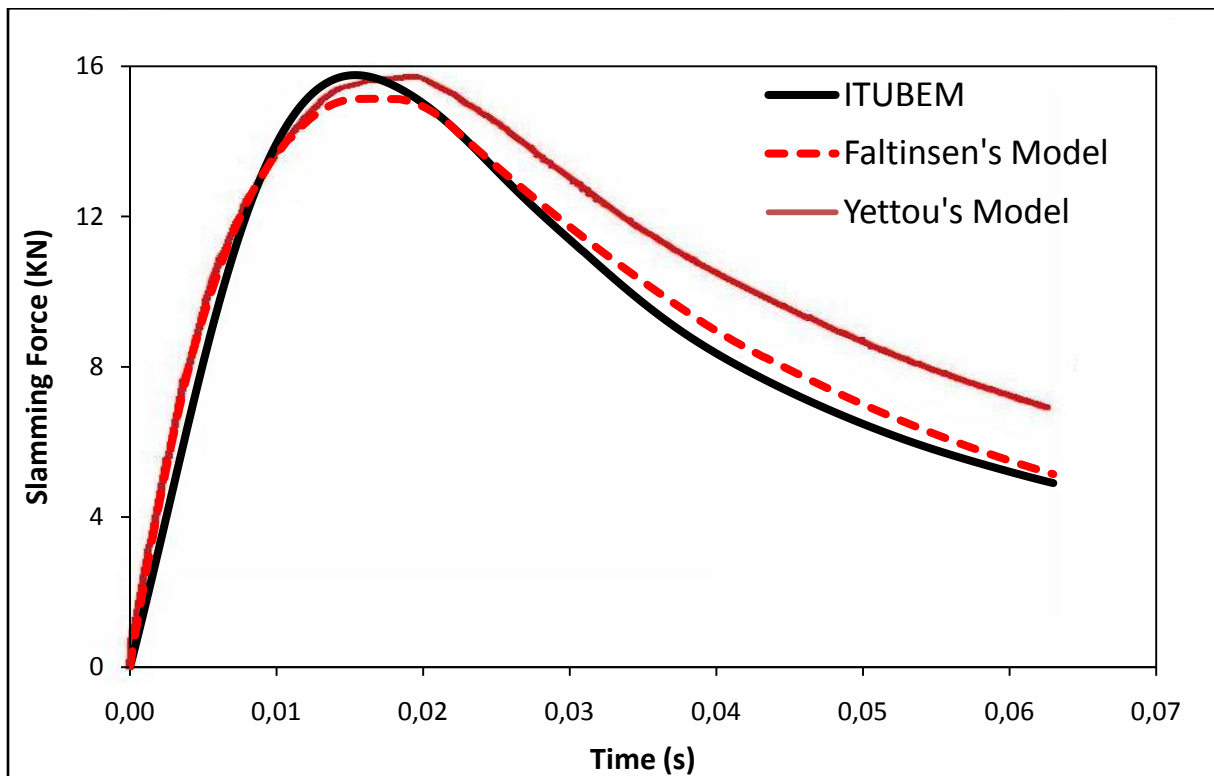


Fig. 10. Comparisons of the resultant slamming forces for a wedge with $\beta = 30^\circ$, $m=153$ kg and drop height is 1.3 m.

Finally, the resultant slamming force of a wedge with 30° deadrise angle at variable downward

velocity has been calculated and compared with Zhao's and Yettou's models. The result of Zhao's

model was calculated by substituting the velocity profile Eq. (18) in Eq. (19). Yettou et al [19] used the same velocity profile to evaluate the pressure. Results were expected to coincide as the acceleration profile of the rigid motion is same. They calculated the resultant slamming force with some difference. The result by ITUBEM shows very good agreement with Zhao's model in the timing, the peak value and the trend.

The developed numerical simulation is capable of being applied to any arbitrary 2-D sections which

increase in width from bottom to upward. For future perspectives, comparisons of results especially with the experiment encourage writers for applying the numerical simulation to a ship bow section in the sense of Strip Theory. In the following step, responses of a ship structure to the symmetrical slamming excitations predicted by ITUBEM can be calculated with or without coupling with the 2-D global motion of a ship travelling in a seaway.

REFERENCES

- [1] **Belik, Ö. Bishop, R.E.D., Price, W.G.**, 1988. Influence of bottom and flare slamming on structural responses. *Trans R Soc London*, Vol.130, 261–275.
- [2] **Bishop, R.E.D., Price, W.D.**, 1979. *Hydroelasticity of Ships*, Cambridge University Press.
- [3] **von Karman, T.**, 1929. The impact on seaplane floats during landing, Technical Notes, National Advisory Committee for Aeronautics.
- [4] **Wagner, H.**, 1932. Über stoss und gleitvorgänge an der oberfläche von flüssigkeiten. *Zeitschrift für Angewandte Mathematik und Mechanik* 12, 192–235.
- [5] **Dobrovolskaya, Z.N.**, 1969, On some problem of similarity flow of flow with a free surface, *Journal of Fluid Mechanics*, Vol.36, pp.805-829.
- [6] **Ochi, M.K. and L.E. Motter**, 1971, A method to estimate Slamming Characteristics for Ship Design, *Marine Technology*, Vol.8, no:2.
- [7] **Stavovy, B.A. and Chuang, S.L.**, 1976, Analytical determination of slamming pressures for high-speed vehicles in waves, *Journal of Ship Research*, Vol.20, No 4, pp 190-198.
- [8] **Zhao R., Faltinsen O.M.**, 1993, Water entry of two-dimensional bodies, *Journal of Fluid Mechanics*, 246:593–612
- [9] **Mei, X., Lui, Y., Yue, D.K.P.**, 1999. On the water impact of general two-dimensional sections. *Applied Ocean Research* 21.
- [10] **Wu, G. X., Sun, H., He, Y. S.**, 2004, Numerical simulation and experimental study of water entry of a wedge in free fall motion, *Journal of fluids and structures*. 19, 277–289
- [11] **Sun, H., Faltinsen, O.M.**, 2007, The influence of gravity on the performance of planing vessels in calm water, *Journal of Engineering Mathematics*, Vol. 58, 91-107.
- [12] **Kihara, H.**, 2008, A numerical study for bow flare slamming analysis using boundary element model, *Proc.6th Osaka Colloquium on Seakeeping and Stability of Ships*, pp.179-186.
- [13] **Gaul L., Kögl M., Wagner M.**, 2003, *Boundary Element Methods for Engineers and Scientists*, Springer-Verlag, Berlin.

- [14] **Greenhow, M.**, 1987, Wedge entry into initially calm water. *App. Ocean Research*, Vol 9, pp 214-223
- [15] **Zhao, R. , Faltinsen, O.M. and Aarsnes, J.**, 1996, Waterentry of arbitrary two-dimensional sections with andwithout flow separation, *Proc. of 21th Symposium onNaval Hydrodynamics*, pp. 408-423
- [16] **Greco, M.**, 2001, A two – dimensional study of green – water loading, *PhD*, NTNU, Trondheim.
- [17] **Sun, H.**, 2007, A boundary element method applied to strongly nonlinear wave – body interaction problems, *PhD*, NTNU, Trondheim.
- [18] **Yettou, E.M., Desrochers, D. and Champoux, Y.**, 2006, Experimental study on the water impact of a symmetrical wedge. *Fluids Dynamics Research*, Vol 38, pp. 47-66.
- [19] **Yettou, E.M., Desrochers, D. and Champoux, Y.**, 2007, A new analytical model for pressure estimation of symmetrical water impact of a rigid wedge at variable velocities. *Journal of Fluid and Structuress* Vol 23, pp. 501-522.
- [20] **Meyerhoff, W.K.**, 1970. Added mass of thin rectangular plates from potential theory. *Journal of Ship Research*, pp. 100-111.